Incremental Force and Moment Coefficients for a Parallel Blade-Vortex Interaction

P. Renzoni* and R. E. Mayle†
Rensselaer Polytechnic Institute, Troy, New York 12181

Blade-vortex interactions occur in helicopter rotors when a rotor blade passes close to or through a tip vortex trailing from the same or another blade. An unsteady, parallel blade-vortex interaction model was developed using a discrete free-vortex method and classical potential flow theory. The tip vortex was modeled by a single vortex and, for a close encounter, by a cluster of vortices. The analysis allows the airfoil to move either steadily or unsteadily through the fluid and allows a freely convecting wake. Comparisons of this nonlinear, unsteady analysis are made with linear airfoil theory for a transient airfoil motion and with linear theory and advanced numerical methods for a two-dimensional parallel interaction problem. The results of numerous blade-vortex calculations are presented, and simple equations are obtained for its incremental force and moment coefficients, which account for interactions at different initial vortex heights, vortex strengths, and airfoil angles of attack. Although the maximum incremental lift coefficient for a close encounter was about four times the dimensionless vortex circulation $\Gamma/U_\infty c$, as calculated using a single vortex representation, its value was about one-third less when the tip vortex was modeled by a cluster of vortices. Comparison with recent experimental results are also presented.

Nomenclature

a = radius of circle in solution plane
C_D = drag coefficient
C_L = lift coefficient
C_M = moment coefficient
C_P = pressure coefficient
c = airfoil chord
K = strength of center vortex in solution plane
K_c = strength of bound vortex
K_g = radius of gyration
K_j = strength of j vortex
p = static pressure
q = magnitude of local velocity
t = time
U = horizontal airfoil velocity
U_∞ = freestream velocity
u = horizontal velocity component
V = vertical airfoil velocity
v = vertical velocity component
W = complex airfoil velocity, $U + iV$
w = complex potential, $\phi + i\Psi$
X = force in the x direction
x = x-coordinate direction
Y = force in the y direction
y = y-coordinate direction
z = complex variable, $x + iy$
α = angle of attack
Γ = circulation of main vortex, $2\pi K_1$
ΔC_L = incremental lift coefficient
ΔC_M = incremental moment coefficient
Δt = time step
ε = airfoil thickness parameter
ε_1 = $1 + \varepsilon$
ζ = complex coordinate in solution plane
ρ = fluid density
ϕ = velocity potential
Ψ = stream function
Ω = airfoil angular velocity

Subscripts

r = relative
te = trailing edge
∞ = freestream value

Received March 6, 1989; revision received Nov. 27, 1989; accepted for publication Dec. 1, 1989.

*Research Assistant, Mechanical and Aeronautical Engineering Department.
†Professor, Mechanical and Aeronautical Engineering Department.

Introduction

In recent years there has been increased interest in the interactions of rotor blades with concentrated tip vortices. Tandem rotors present many situations in which these interactions can occur, but even single rotor helicopters experience these interactions under certain flight conditions. Egolf and Landgrebe[1] have indicated that close blade-vortex interactions occur for low and moderate forward flight speed conditions at low advance ratios where the movement of the tip vortices above and then down through the rotor disk result in blade-vortex impingement. In addition, blade-vortex interactions are believed to be responsible for the high impulsive noise associated with rotorcraft during low-power descending flight and maneuvers. Under these conditions, as shown by Charles[2] and Pegg[3], concentrated tip vortices are blown back into the rotor disk resulting in numerous interactions. These encounters cause large, unsteady impulsive aerodynamic loads on the rotor blades and are one of the mechanisms responsible for the high frequency noise commonly referred to as blade slap. An accurate modeling of this problem is essential to the accurate prediction of rotor air loads and performance.

The general blade-vortex interaction problem is three dimensional and unsteady, and the curved-line vortex intersects the blade at various angles. Although oblique interactions represent the helicopter application more closely, two limiting cases of interactions are of fundamental interest. One limiting case occurs when the axis of the vortex is aligned with the freestream direction and the vortex is normal to the blade leading edge. Another occurs when the axis of the vortex is parallel to the blade leading edge. The interaction between an oblique infinite vortex with a blade in a parallel plane was

first considered by Widnall,[4] who used linearized flow theory and represented the velocity field of the vortex as a distribution of oblique sinusoidal gusts using Fourier transforms. An analyis of the acoustic field showed that parallel interactions produced the highest amplitude pulse. This result was supported by the experimental results of Nakamura.[5] Acoustic measurements for a model rotor by Martin et al.[6] have located the source of primary blade-vortex interaction noise at an angle between 70 and 90 deg azimuth where nearly parallel interactions occur. Although impulsive pressure disturbances have been observed in blade surface pressure data in the retreating side by Hubbard and Leighton,[7] no blade-vortex interaction noise on the retreating side was found. Since a parallel interaction affects a larger span of the blade than a perpendicular interaction, it is reasonable to expect that a model for the parallel interaction is more crucial to predicting blade forces and moments during blade-vortex interactions.

The parallel blade-vortex interaction problem was first looked at by Sears[8] using classical, incompressible, two-dimensional unsteady airfoil theory. The lift on the blade was calculated from the gust-entry lift function of von Karman and Sears[9] using Duhamel superposition. As the vortex approaches the blade leading edge, the lift approaches a peak and then overshoots and asymptotically approaches the steady value from above as the vortex moves away from the blade. In the linear theory of Sears, the vortex is kept at a constant vertical distance from the blade during the encounter. Parthasarathy[10] and Chow and Huang[11] have solved the incompressible problem using conformal mapping techniques in which the vortex is convected at the local velocity. The theory of Parthasarathy forces the wake vorticity to move at the freestream velocity, whereas Chow and Huang allow the wake vorticity to move at the local induced velocity. Chow and Huang apply their theory to the problem of capturing a vortex to increase the lifting capabilities of an airfoil. Conformal mapping techniques have also been used by Meyer and Timm,[12] Panaras,[13] and Poling et al.[14] Meyer and Timm do not satisfy the Kutta condition at the blade trailing edge, whereas Panaras satisfies the condition by setting the circulation of the blade and not by shedding vorticity at the trailing edge. Poling et al. satisfied the Kutta condition by shedding vorticity from the blade trailing edge but incorrectly evaluated the temporal change of the potential function in Bernoulli's equation. As a result, their calculations did not compare well with other conventional panel methods to represent the surface of the airfoil. They have also decomposed the loads on the airfoil in various physical components. Viscous interactions have been analyzed only recently. Hardin and Lamkin[16] and Wu et al.[15,17] have solved the full Navier-Stokes equations in the vorticity-stream function form. Hardin and Lamkin have only looked at a Reynolds number of 2×10^2, whereas Wu et al. have examined flows with Reynolds numbers of 1×10^5 and 1×10^6.

The parallel interaction problem was first analyzed in transonic flow by Caradonna et al.[18] and McCroskey and Goorjian[19] using the unsteady transonic small disturbance theory. Jones[20] and Sankar and Malone[21] have modeled the interaction more accurately by applying the full potential equation without any small disturbance or low-frequency assumptions. Srinivasan et al.[22–24] and Wu et al.[17] have developed more advanced interaction models by solving the unsteady Euler equations and the unsteady, time-averaged, compressible Navier-Stokes equations. All of these advanced analyses are rather time consuming to perform and are not, as yet, convenient for use within current helicopter design systems.

In the present study, the parallel blade-vortex interaction is analyzed using simple incompressible potential flow theory with the thought of establishing a useful framework for which the problem could be viewed by a designer. Although the theory presented below could be incorporated into an existing design system without significantly increasing computer execution time, the first goal was to obtain a simple set of correlations for the incremental changes in lift, drag, and moment caused by the interaction.

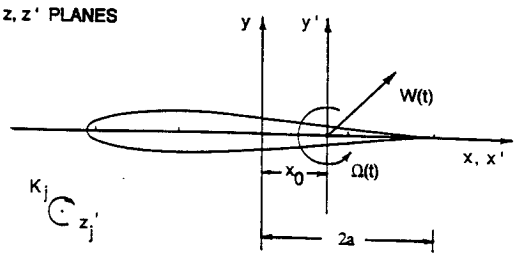

Fig. 1 Blade-vortex interaction in a moving coordinate system.

Theoretical Analysis

A generalized theory for the interaction of discrete vortices with a symmetric Joukowski airfoil in unsteady motion is considered. Figure 1 shows the airfoil fixed to a coordinate system x', y', which is translating with a complex velocity $W(t) = U(t) + iV(t)$ and rotating with an angular velocity $\Omega(t)$. The tip vortex and the wake behind the airfoil are modeled by discrete vortices. The theory is applied step by step in time along the airfoil flight path. At every time step, the vorticity that is shed into the wake is represented by a newly formed discrete vortex.

The symmetric Joukowski airfoil in a z plane is mapped into a circle of radius a in the ζ plane by the transformations,

$$z' = z - x_0, \qquad z = \zeta' + \frac{a^2}{\zeta'}, \qquad \text{and} \quad \zeta' = \varepsilon_1 \zeta - \varepsilon a \tag{1}$$

The details of the mapping are shown in Fig. 2.

A body of arbitrary shape moving unsteadily in a still fluid generates a disturbance potential that is a function of the body shape and the unsteady motion. Milne-Thomson[25] has presented a method by which the complex disturbance potential is determined for a body of any shape provided it can be mapped into a circle. The complex disturbance potential for the flow of N vortices over a moving Joukowski airfoil in the z' plane is given in the ζ plane by

$$\begin{aligned} w(\zeta) &= \phi + i\psi \\ &= (\bar{W} + i\Omega x_0)\frac{a^2}{\zeta'} - \varepsilon_1 (W - i\Omega x_0)\frac{a^2}{\zeta} \\ &\quad - i\Omega a^3\left[-\frac{\varepsilon\varepsilon_1}{\zeta} + \frac{a\varepsilon_1}{\zeta\zeta'} - \frac{\varepsilon}{\zeta'}\right] + iK\ell n\,\zeta \\ &\quad + i\sum_{j=1}^{N} K_j\left[\ell n(\zeta - \zeta_j) - \ell n\left(\zeta - \frac{a^2}{\bar{\zeta}_j}\right)\right] \end{aligned} \tag{2}$$

where ϕ and Ψ are the disturbance potential and disturbance stream functions, respectively, and where $\bar{W}$ is the complex conjugate of the velocity W. The strength of the vortex at the center of the circle in the ζ plane K is given by

$$K(t) = K_c(t) + \sum_{j=1}^{N} K_j \tag{3}$$

where K_c is the strength of the circulation around the airfoil (circle).

The complex disturbance velocity at all points in the flow other than the center of the discrete vortices and at the trailing edge relative to the moving x', y' coordinate system is obtained by differentiating Eq. (2). Denoting the relative velocity as q_r, one obtains

$$q_r = u_r - iv_r = \frac{dw}{dz'} - (\bar{W} - i\Omega\bar{z}') = \frac{dw}{d\zeta}\frac{d\zeta}{dz'} - (\bar{W} - i\Omega\bar{z}') \tag{4}$$

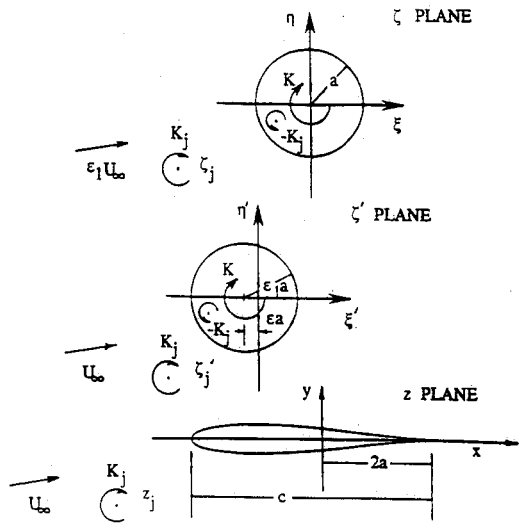

Fig. 2 Mapping the flow about a symmetric Joukowski airfoil into the circle plane.

where

$$\frac{dw}{d\zeta} = -\varepsilon_1(\bar{W} + i\Omega x_0)\frac{a^2}{\zeta'^2} + \varepsilon_1(W - i\Omega x_0)\frac{a^2}{\zeta^2} - i\Omega a^3\left[\frac{\varepsilon\varepsilon_1}{\zeta^2} - \frac{2a\varepsilon_1}{\zeta^2\zeta'} - \frac{a^2\varepsilon\varepsilon_1}{\zeta^2\zeta'^2} + \frac{\varepsilon\varepsilon_1}{\zeta'^2}\right] + i\frac{K}{\zeta} + i\sum_{j=1}^{N} K_j\left[\frac{1}{(\zeta - \zeta_j)} - \frac{\bar{\zeta}_j}{(\zeta\bar{\zeta}_j - a^2)}\right]$$

$$\frac{d\zeta}{dz'} = \frac{d\zeta}{d\zeta'}\frac{d\zeta'}{dz}\frac{dz}{dz'} = \frac{\zeta'^2}{\varepsilon_1(\zeta'^2 - a^2)} \tag{5}$$

The induced complex disturbance velocity of the jth vortex in the solution plane is given by

$$\left(\frac{dw}{d\zeta}\right)_j = \frac{d}{d\zeta}[w(\zeta) - iK_j \ell n(\zeta - \zeta_j)]_{\zeta=\zeta_j} = \left[\frac{dw}{d\zeta} - i\frac{K_j}{(\zeta - \zeta_j)}\right]_{\zeta=\zeta_j} \tag{6}$$

The induced complex disturbance velocity of the jth vortex in the physical plane, however, is obtained from the expression

$$\left(\frac{dw}{dz'}\right)_j = \frac{d}{d\zeta}[w(\zeta) - iK_j \ell n(z - z_j)]_{\zeta=\zeta_j}\left(\frac{d\zeta}{d\zeta'}\right)_{\zeta=\zeta_j}\left(\frac{d\zeta'}{dz}\right)_{\zeta=\zeta_j} = \left(\frac{dw}{d\zeta}\right)_j\frac{\zeta_j'^2}{\varepsilon_1(\zeta_j'^2 - a^2)} - iK_j\frac{a^2\zeta_j'}{(\zeta_j'^2 - a^2)^2} \tag{7}$$

Then the relative induced complex velocity of the jth vortex is

$$(q_r)_j = \left(\frac{dw}{d\zeta}\right)_j\frac{\zeta_j'^2}{\varepsilon_1(\zeta_j'^2 - a^2)} - iK_j\frac{a^2\zeta_j'}{(\zeta_j'^2 - a^2)^2} - (\bar{W} - i\Omega\bar{z}_j') \tag{8}$$

The velocity at the cusped trailing edge is determined by imposing the Kutta condition. To have a finite velocity at the airfoil's trailing edge, a stagnation point is situated at the point in the solution plane that maps into the trailing edge. This requires that

$$\left(\frac{dw}{d\zeta}\right)_{\zeta=a} = 0 \tag{9}$$

Applying the preceding condition to Eq. (5) gives the expression for the strength of the vortex at the center of the solution plane as

$$K(t) = -2a\varepsilon_1 V(t) + 2a\varepsilon_1 x_0\Omega(t) + a^2\varepsilon_1(\varepsilon - 2)\Omega(t) - \sum_{j=1}^{N} K_j\frac{a^2 - \zeta_j\bar{\zeta}_j}{(a - \zeta_j)(a - \bar{\zeta}_j)} \tag{10}$$

At the trailing edge, Eq. (9) is indeterminate, and the complex velocity is calculated using L'Hospital's rule. Substituting the preceding expression into the resulting expression yields a relative velocity at the trailing edge of

$$(q_r)_{te} = (u_r)_{te} = -\frac{U}{\varepsilon_1} + \frac{i}{2\varepsilon_1^2}\sum_{j=1}^{N} K_j\left[\frac{-\zeta_j}{(a - \zeta_j)^2} + \frac{\bar{\zeta}_j}{(a - \bar{\zeta}_j)^2}\right] \tag{11}$$

At each time step, the problem is well defined by Eqs. (1–11). The only two unknowns are the location and the strength of the shed vortex. In the present analysis, the shed vortex is positioned downstream of the trailing edge in the physical z plane at

$$x_N(t) = 2a + (u_r)_{te}\Delta t, \qquad y_N(t) = 0 \tag{12}$$

where $(u_r)_{te}$ is the relative trailing edge velocity at time $t - \Delta t$. The strength of the shed vortex is determined by requiring that the total circulation be conserved at all times. When there are initially m vortices in the flow, conservation of circulation requires that

$$K_c(t = 0) + \sum_{j=1}^{M} K_j = K_c(t) + \sum_{j=1}^{N} K_j \tag{13}$$

From Eq. (3), this provides $K(t = 0) = K(t) = \text{const}$.

Although the strength of the circulation about the airfoil $K_c(t)$ varies with time, the strength of the vortex at the center of the circle $K(t)$ remains constant. $K(t)$ is evaluated from Eq. (10) at $t = 0$ when all of the terms on the right-side are known. At time t, the shed vortex strength K_N is determined from Eq. (10) as

$$K_N = \left[2a\varepsilon_1(V - \Omega x_0) - a^2\varepsilon_1(\varepsilon - 2)\Omega + K + \sum_{j=1}^{N-1} K_j\frac{a^2 - \zeta_j\bar{\zeta}_j}{(a - \zeta_j)(a - \bar{\zeta}_j)}\right]\left[\frac{\zeta_N\bar{\zeta}_N - a^2}{(a - \zeta_N)(a - \bar{\zeta}_N)}\right]^{-1} \tag{14}$$

The pressure at a point z' is determined through the unsteady Bernoulli equation. In a moving coordinate system, the pressure coefficient is expressed by[25]

$$C_p = \frac{p - p_\infty}{\rho U_\infty^2/2} = \left(\frac{\bar{W}}{U_\infty} + i\frac{\Omega z'}{U_\infty}\right)\left(\frac{\bar{W}}{U_\infty} - i\frac{\Omega\bar{z}'}{U_\infty}\right) - \left(\frac{q_r}{U_\infty}\right)^2 - \frac{2}{U_\infty^2}\frac{\partial\phi}{\partial t} \tag{15}$$

where q_r is evaluated from Eq. (4) and the unsteady term is derived by differentiating Eq. (2) such that

$$\frac{\partial\phi}{\partial t} = \frac{\partial\phi}{\partial t_{nc}} + \frac{\partial\phi}{\partial t_c} \tag{16}$$

in which the noncirculatory component, sometimes referred to as apparent mass, is

$$\frac{\partial\phi}{\partial t_{nc}} = \text{Real}\left\{\left[\frac{d\bar{W}}{dt} + ix_0\frac{d\Omega}{dt}\right]\frac{a^2}{\zeta'} - \varepsilon_1\left[\frac{dW}{dt} - ix_0\frac{d\Omega}{dt}\right]\frac{a^2}{\zeta} - ia^3\left[-\frac{\varepsilon\varepsilon_1}{\zeta} + \frac{a\varepsilon_1}{\zeta\zeta'} - \frac{\varepsilon}{\zeta'}\right]\frac{d\Omega}{dt}\right\} \tag{17}$$

and the circulatory component is

$$\frac{\partial \phi}{\partial t_c} = \text{Real}\left\{ -i \sum_{j=1}^{N} \frac{K_j}{(\zeta - \zeta_j)} \frac{d\zeta_j}{dt} + i \sum_{j=1}^{N} \frac{a^2 K_j}{\bar{\zeta}_j (a^2 - \zeta \bar{\zeta}_j)} \frac{d\bar{\zeta}_j}{dt} \right\} \quad (18)$$

The forces and moments acting on the airfoil may be evaluated from the unsteady Blasius theorem. In a moving coordinate system, the unsteady Blasius theorem is expressed as

$$X - iY = i\frac{\rho}{2}\int_c \left(\frac{dw}{dz'}\right)^2 dz' - \rho\Omega \int_c \bar{z}'\, dw + i\rho \frac{\partial}{\partial t}\int_c \bar{w}\, d\bar{z}' + 2\pi i \rho K_c \bar{W} - i\rho A\left[-\Omega(\bar{W} - i\Omega \bar{z}'_c) + i\left(\frac{d\bar{W}}{dt} - i\bar{z}'_c \frac{d\Omega}{dt}\right)\right] \quad (19)$$

and

$$M_0 = \text{Real}\left\{ -\frac{\rho}{2}\int_c z'\left(\frac{dw}{dz'}\right)^2 dz' + \rho \bar{W} \int_c z'\, dw - \rho\Omega A \bar{W} z'_c - \rho \frac{\partial}{\partial t_c}\int_c z' w\, d\bar{z}' - \rho A\left[3iz'_c \frac{d\bar{W}}{dt} + 2K_g^2 \frac{d\Omega}{dt}\right]\right\} \quad (20)$$

where X and Y are the forces per unit span acting parallel and normal to the airfoil, respectively, and M_0 is the moment about the origin in the x', y' coordinate system positive in the counterclockwise direction. Equations (19) and (20) are computationally more efficient than numerical integration and are also applicable when the airfoil is a flat plate.

Calculation Procedure

The blade-vortex interaction problem is characterized by the time history of the airfoil motion, the airfoil thickness parameter ε, and the strength of the initial vortices and their location in the physical plane. The calculation begins by mapping the initial vortices into the solution plane and calculating the center vortex strength K from Eq. (10). This value of K remains constant throughout the calculation. The relative induced velocities of the initial vortices and the relative trailing-edge velocity are calculated using Eqs. (8) and (11), respectively.

Having established the initial problem, the initial vortices are convected in the flow, and a discrete vortex is shed from the trailing edge into the wake at each time step. At a time t, there are N-1 vortices in the flowfield from the previous time step, and a new vortex is shed into the wake. Equations (12) and (14) are used to determine the location and strength of the Nth vortex. The strength of the shed vortex remains constant throughout the remaining calculations as it is convected downstream. The relative induced velocities of the N vortices are computed from Eq. (8), and the vortices are advanced to their position at time $t + \Delta t$ through the following backward difference expression

$$z_j(t + \Delta t) = z_j(t) + \tfrac{1}{2}[3(\bar{q}_r)_j(t) - (\bar{q}_r)_j(t - \Delta t)]\Delta t \quad (21)$$

that has been written for a typical jth vortex. This expression is found to be better than straight extrapolation, especially in close encounters with the airfoil and with one another, where the vortices move rapidly. The relative velocity at the trailing edge is calculated at time t so that the position of the new shed vortex at time $t + \Delta t$ may be determined. At all time steps, the pressure distribution, forces, and moment are determined from Eqs. (15), (19), and (20).

Discussion of Results

A comparison of the present calculation method to the linear theory for a flat plate, initially at zero angle of attack, and pitched linearly to another angle about its quarter-chord is shown in Fig. 3. In this case, the final angle of attack of 0.1 rad was obtained after a nondimensional time $U_\infty t/c = 0.5$. The wake generated by this motion is shown above the lift coefficient plot. One should note that the discrete vortex analysis shows two vortex clusters are produced by this motion—one having positive circulation and the other negative. The linear theory consists of a Duhamel integration of Wagner's function,[26] which gives the growth of circulation

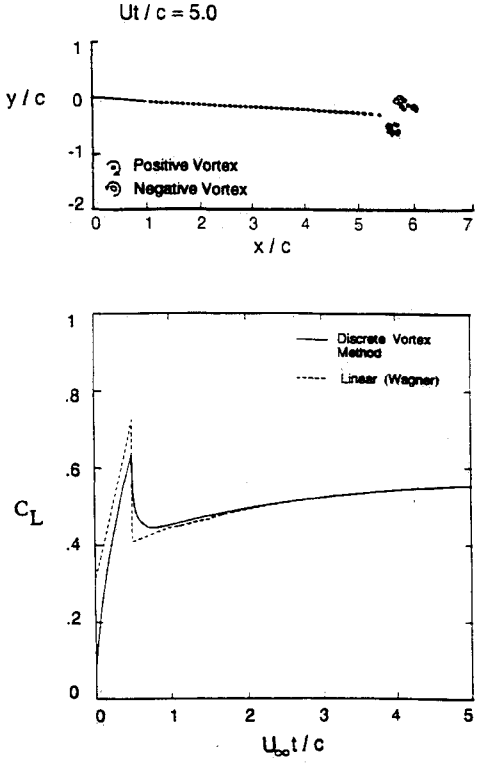

Fig. 3 Comparison with linear theory for a transient motion.

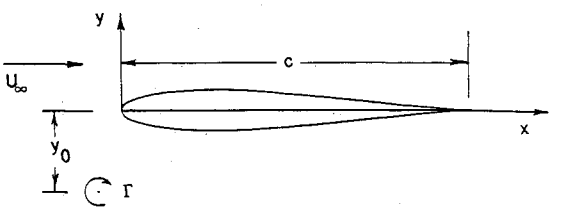

Fig. 4 Description of a simple parallel blade-vortex interaction.

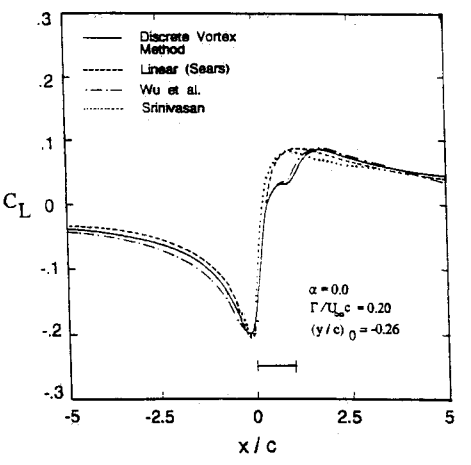

Fig. 5 Comparison with other inviscid blade-vortex analyses.

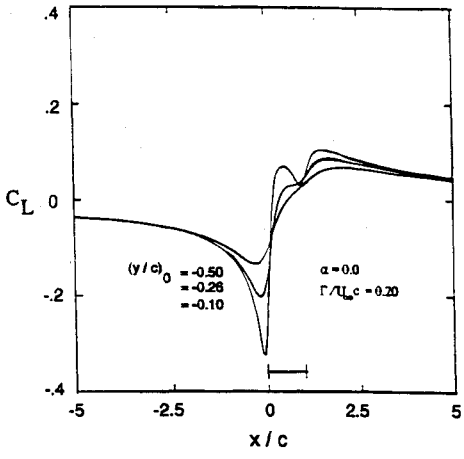

Fig. 6 Effect of initial vortex height on lift coefficient, $\Gamma/U_\infty c = 0.2$.

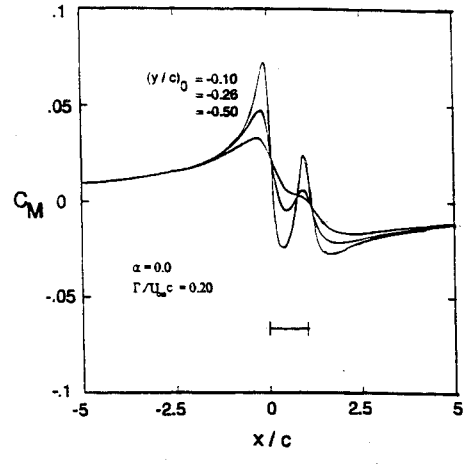

Fig. 7 Effect of initial vortex height on moment coefficient, $\Gamma/U_\infty c = 0.2$.

about the airfoil due to a sudden increase in downwash, which is uniform over the airfoil. The sudden jumps seen in Fig. 3 reflect the inability of the linear theory to handle the sudden, finite jumps in angular velocity created by the ramp profile. The response of the discrete vortex method, while similar to that of the linear theory, is somewhat smoother as one should expect. The agreement betwen the two is quite good after the second discontinuity. A comparison of the discrete vortex method to the linear theory of Theodorsen[27] for a flat plate plunging sinusoidally was shown to be in a good agreement by Straus et al.[28]

Wu et al.[15] and Srinivasan and McCroskey[24] have analyzed the simple blade-vortex interaction problem shown in Fig. 4 using different inviscid methods of analyses. For this problem, a vortex having a circulation $\Gamma/U_\infty c = 0.2$ (positive in the clockwise direction), initially placed below the airfoil at $(y/c)_0 = -0.26$, passes a NACA 0012 airfoil at zero angle of attack. Their results together with the results from the present discrete vortex method and the linear theory of Sears[8] are presented in Fig. 5 where the lift coefficient during the encounter is plotted against the streamwise position of the vortex. The airfoil lies between $x/c = 0$ and 1 as shown by the horizontal line in the figure. For the present analysis, an 11.5% symmetric Joukowski airfoil, which closely models the NACA airfoil, was used. The analysis of Srinivasan and McCroskey is for compressible flow, but their result is shown for a Mach number equal to 0.3 where the compressibility effects are expected to be minor. It should be noted, however, that they used a small disturbance theory. Wu et al. used potential flow theory.

In general, all of the analyses predict nearly the same trend

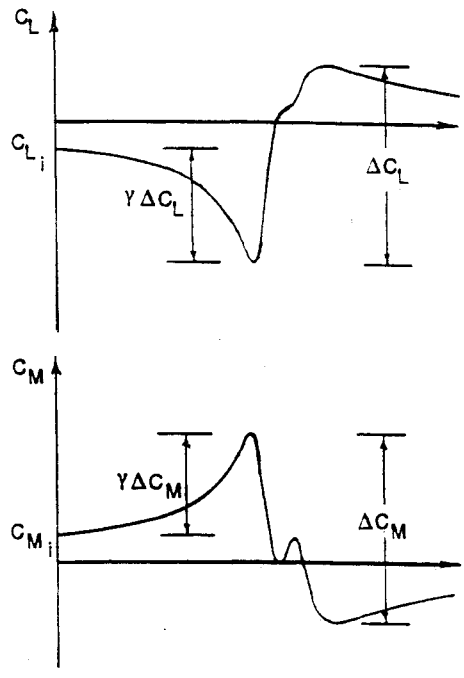

Fig. 8 Definition of incremental lift and moment coefficients.

and disturbance amplitudes during the encounter. When the vortex is in front of the airfoil $x/c < 0$, it produces a flow with a negative angle of attack (see Fig. 4), which in turn causes a lift in the negative direction. Once aft of the airfoil, the effective angle of attack is positive and so is the lift. As the vortex passes over the airfoil, the pressures depend not only on the position of the vortex, but on the rate of change of its position. This gives rise to the rapid change from the negative to positive lift observed in Fig. 5 in this region. Most importantly, however, the present discrete vortex method and the analysis of Wu et al. are virtually identical. This is not surprising, since the only difference between the two methods is that Wu et al. represents the airfoil surface using vortex segments, and the present method uses a continuous airfoil. An interesting feature of the interaction is that the vortex has a long range effect in that the lift varies when the vortex is both far upstream and downstream from the airfoil. The small discrepancies between all of the results for $x/c < 0$ presumably arise from slightly different starting conditions used in each analysis. For this calculation, the vortex was initially placed at $x/c = -5.8$ and $y/c = -0.26$. When the vortex is immediately below the airfoil ($0 \leqslant x/c \leqslant 1$), the small disturbance analysis of Srinivasan and McCroskey and the linear airfoil theory of Sears behave identically, but noticeably different than the nonlinear potential flow analysis.

In the general blade-vortex interaction problem, the vortex encounters the blade under numerous conditions. For a parallel interaction, such as shown in Fig. 4, the important variables of the problem are the initial position of the vortex above (or below) the airfoil $(y/c)_0$, the nondimensional vortex circulation $\Gamma/U_\infty c$, and the angle of attack α. The discrete vortex method was used to study the blade-vortex interaction problem under a wide range of these variables. In particular, the initial vortex height $(y/c)_0$ was varied from -1 to $+1$, vortex circulations $\Gamma/U_\infty c$ from 0.1 to 0.4 were considered, and the angle of attack was varied from 0 to 4 deg. All calculations were started at $(x/c)_0 = -5.8$. In each case, the lift, moment, and drag coefficients C_L, C_M, and C_D, respectively, were calculated. Representative samples of the results are shown in Figs. 6 and 7 where the effect of the initial vortex height $(y/c)_0$ is shown. Each figure contains the results for $\Gamma/U_\infty c = 0.2$ and $\alpha = 0$. As expected, the close encounters result in large fluctuations in the aerodynamic coefficients. Far upstream and downstream of the airfoil, the results are

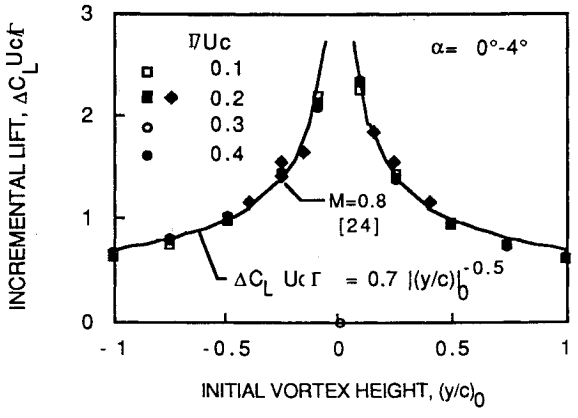

Fig. 9 Correlation of the incremental lift coefficient.

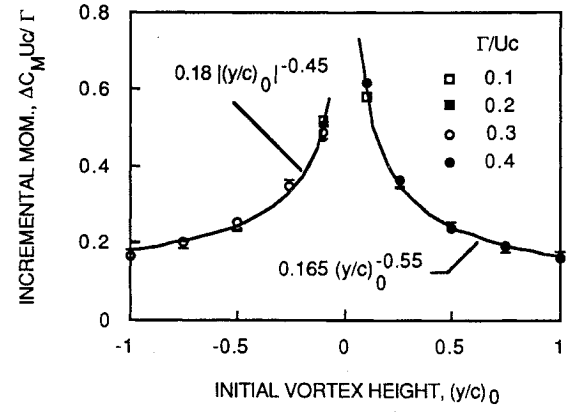

Fig. 10 Correlation of the incremental moment coefficient.

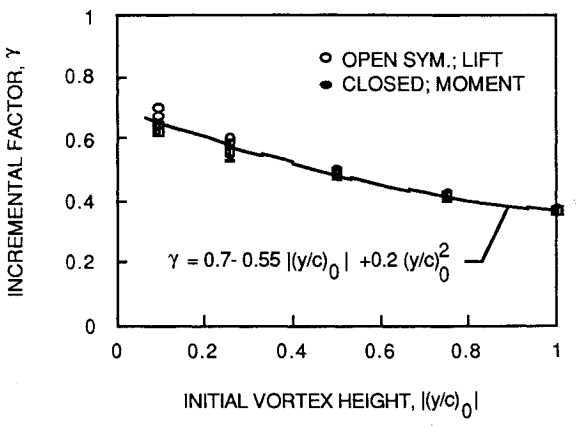

Fig. 11 Correlation of the incremental factor.

virtually identical. In fact, for the same height above and below the airfoil, the results are almost identical up to the point where the vortex is in line with the leading edge. As the vortex passes the airfoil, larger differences become apparent. The drag is largely negative (vortex exerts a forward thrust on the airfoil) during the entire interaction for all conditions with a maximum excursion less than 8% of the excursion in lift.

The results for all conditions were very similar in that they all exhibit very strong peaks during the interaction, which was in general related to the strength of the vortex and its initial height relative to the airfoil. This feature allowed one to express the overall behavior of all of the results in a very simple and convenient form by defining incremental force and moment coefficients. Typical curves showing the incremental lift and moment coefficients ΔC_L and ΔC_M, respectively, and an incremental factor γ are shown in Fig. 8. It was found that these incremental coefficients were nearly proportional to the vortex circulation $\Gamma/U_\infty c$. In Fig. 9, a corrected incremental lift coefficient $\Delta C_L(U_\infty c/\Gamma)$ is plotted against the initial vortex height $(y/c)_0$ for various values of $\Gamma/U_\infty c$. All of the results can be calculated quite well by the equation

$$\Delta C_L = 0.7 \frac{\Gamma}{U_\infty c\sqrt{|(y/c)_0|}}; \qquad (y/c)_0 \neq 0 \tag{22}$$

This relation appears to be adequate for both $(y/c)_0 > 0$ and $(y/c)_0 < 0$ and for angles of attack between 0 and 4 deg with a vortex circulation $\Gamma/U_\infty c = 0.2$. For an interaction with an airfoil at an angle of attack, the incremental coefficients represent only the changes caused by the passing vortex. Srinivasan and McCroskey have calculated temporal lift distributions for incident Mach numbers of 0.3 and 0.8. As can be seen from Fig. 5 for the Mach number of 0.3 and from Fig. 9 for 0.8, their results are virtually identical with the calculation by the discrete vortex method.

The results for the incremental moment coefficient are shown in Fig. 10. In this case, the results for a vortex passing below the airfoil are somewhat different than those for a vortex passing above and require separate correlations, namely

$$\Delta C_M = \begin{cases} 0.18|(y/c)_0|^{-0.45} \dfrac{\Gamma}{U_\infty c}; & (y/c)_0 < 0 \\ 0.165(y/c)_0^{-0.55} \dfrac{\Gamma}{U_\infty c}; & (y/c)_0 > 0 \end{cases} \tag{23}$$

As will be seen, these relations together with that for the incremental lift coefficient must be modified near $(y/c)_0 = 0$ to account for a finite vortex size.

The incremental factor γ is plotted in Fig. 11 for both the lift and moment results. Since the results for both positive and negative values of $(y/c)_0$ were nearly the same, the results for both are plotted using the same coordinate. It is seen that the differences between the incremental factor for the lift and moment are slight and that the results can be calculated reasonably well by

$$\gamma = 0.7 - 0.55|(y/c)_0| + 0.2(y/c)_0^2 \tag{24}$$

For an interaction with a vortex having a positive circulation, the lift first decreases and the moment increases by an amount $\gamma\Delta C_L$ and $\gamma\Delta C_M$, respectively. As the vortex passes over the airfoil, the lift then increases and the moment decreases by an amount ΔC_L and ΔC_M (see Figs. 9 and 10). This last change occurs over a distance of about 1–2 chord lengths.

The results for the incremental drag coefficient have not been shown but can be calculated quite well by the equation

$$\Delta C_D/\Delta C_L = 0.030\left(\frac{\Gamma}{U_\infty |y_0|}\right)^{0.75}; \qquad y_0 \neq 0 \tag{25}$$

which provides a maximum excursion less than 10% of the incremental lift coefficent for $\Gamma/U_\infty|y_0| \leq 5$.

Equations (22–25) then provide a relative simple set of equations for the incremental force and moment coefficients that can be used in helicopter design. Difficulties arise in using these, however, for either very close encounters or when the vortex causes the airfoil to separate. For very close encounters, representing the main vortex by a single discrete vortex is unrealistic. In this case, the vortex is best represented by a cluster of single vortices positioned initially in the core of the main vortex. Calculations were done for a main vortex composed of a cluster of 20 discrete vortices within a core of diameter $0.1c$ and compared to the results using a single main vortex. The interested reader is referred to Renzoni[29] for further details. In each case, the circulation around the single vortex and the clustered vortices was $\Gamma/U_\infty c = 0.16$. The

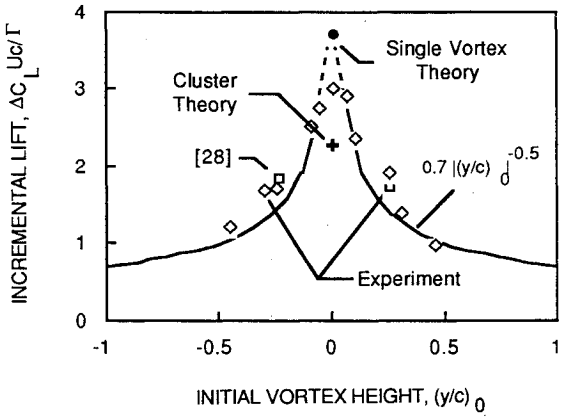

Fig. 12 Incremental lift coefficient for a close encounter and comparisons with experiments.

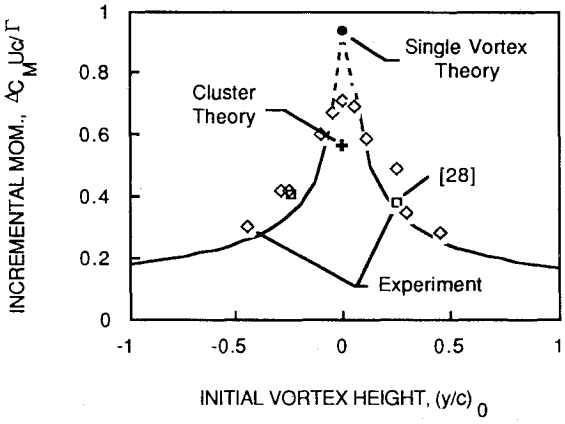

Fig. 13 Incremental moment coefficient for a close encounter and comparisons with experiments.

comparisons of the incremental lift and moment coefficients for an initial vortex height $(y/c)_0 = 0$ at zero angle of attack are shown in Figs. 12 and 13, resepctively. For both the lift and moment, the incremental coefficient for the cluster vortex is about one-third lower than that predicted by the single vortex. As shown by Renzoni, the composite vortex for this encounter acutally splits into two separate clusters and passes both above and below the airfoil. This produces a drastically reduced excursion in pressure as the vortex pairs pass over the airfoil and consequently reduces the incremental lift and moment coefficients. Apparently, as can be seen from the figures, a single vortex theory is not appropriate for encounters having an initial height $(y/c)_0$ less than ± 0.1–0.2.

The latest experimental results from tests conducted at Rensselaer Polytechnic Institute are also shown in Figs. 12 and 13. The results presented in Straus et al.,[28] corrected for proper $(y/c)_0$ and vortex strength, are also presented. The data are for a vortex with circulations $\Gamma/U_\infty c$ between 0.1 and 0.14. The agreement between the theory and experiment is encouraging. Interestingly, the experimental results near zero interaction height fall between those for the single and cluster-vortex calculations.

Conclusions

A discrete vortex, potential flow method was developed to evaluate the blade-vortex interaction problem where the airfoil is allowed to move either steadily or unsteadily through the fluid. A comparison with linear theory for a small-amplitude transient for a linearly pitched airfoil showed that the discrete vortex method yields a more reasonable lift history distribution. Whereas a comparison for the blade-vortex interaction problem with another potential flow calculation showed excellent agreement, small discrepancies were noted when the blade-vortex interaction problem was compared to some small-perturbation, inviscid results.

Calculations for a parallel blade-vortex interaction were performed for a variety of initial vortex positions, vortex strengths, and airfoil angles of attack. It was found that the main features of the lift, drag, and moment results during the interaction could be characterized by incremental coefficients, which varied directly with the vortex circulation $\Gamma/U_\infty c$ and roughly inversely to the square root of the initial distance between the vortex and the airfoil, $(\sqrt{|(y/c)_0|})^{-1}$.

Finally, comparisons with an analysis using a cluster of vortices to represent the trailing tip vortex and with recent experimental results showed reasonable agreement. Although further work may be necessary for close interactions where the vortex splits, it appears that a simple inviscid theory is sufficient to evaluate the effects of a passing vortex on airfoil forces and moments in most encounters. It also appears that an incompressible calculation using a single potential vortex is quite adequate.

Acknowledgment

This work was sponsored by the Army Research Office through the Rotorcraft Center at Rensselaer Polytechnic Institute under Contract DAAG29-92-K-0093. The authors are indebted to J. Straus for the results shown in Figs. 12 and 13.

References

[1]Egolf, T. A., and Landgrebe, A. J., "Helicopter Rotor Wake Geometry and Its Influence in Forward Flight—Volume I—Generalized Wake Effects on Rotor Airloads and Performance," NASA CR-3726, 1983.

[2]Charles, B. D., "Acoustic Effects of Rotor-Wake Interaction During Low-Power Descent," *American Helicopter Society Symposium on Helicopter Aerodynamic Efficiency*, 1975.

[3]Pegg, R. J., "A Summary and Evaluation of Semi-Empirical Methods for the Prediction of Helicopter Rotor Noise," NASA TM-80200, 1979.

[4]Widnall, S., "Helicopter Noise due to Blade-Vortex Interaction," *Journal of the Acoustical Society of America*, Vol. 50, No. 1, 1971, pp. 354–365.

[5]Nakamura, Y., "Prediction of Blade-Vortex Interaction from Measured Blade Pressure Distributions," *Seventh European Rotorcraft and Powered Lift Aircraft Forum*, Vol. 1, Deutsche Gesellschaft für Luft: and Raumfahrt e. V., Paper 32, 1981, pp. 32-1 to 32-19.

[6]Martin, R. M., Elliott, J. W., and Hoad, D. R., "Experimental and Analytic Predictions of Rotor Blade Vortex Interaction," *Journal of the American Helicopter Society*, Vol. 31, No. 4, 1986, pp. 12–20.

[7]Hubbard, J. E., Jr., and Leighton, K. P., "A Comparison of Model Helicopter Rotor Primary and Secondary Blade/Vortex Interaction Blade Slap," AIAA Paper 83-0723, April 1983.

[8]Sears, W. R., "Aerodynamics, Noise, and the Sonic Boom," *AIAA Journal*, Vol. 7, No. 4, 1969, pp. 577–586.

[9]von Karman, T., and Sears, W. R., "Airfoil Theory for Non-Uniform Motion," *Journal of the Aeronautical Sciences*, Vol. 5, No. 10, 1938, pp. 379–390.

[10]Parthasarathy, R., "Aerodynamic Sound Generation due to Vortex-Airfoil Interaction," Ph.D. Dissertation, Stanford Univ., Stanford, CA, 1972.

[11]Chow, C.-Y., and Huang, M.-K., "Unsteady Flows about a Joukowsky Airfoil in the Presence of Moving Vortices," AIAA Paper 83-0129, Jan. 1983.

[12]Meyer, G. E. A., and Timm, R., "Unsteady Vortex Airfoil Interaction," AGARD CP-386, 1985.

[13]Panaras, A. G., "Numerical Modeling of the Vortex/Airfoil Interaction," *AIAA Journal*, Vol. 25, No. 1, 1987, pp. 5–11.

[14]Poling, D. R., Dadone, L., and Telionis, D. P., "Blade-Vortex Interaction," *AIAA Journal*, Vol. 27, No. 6, pp. 694–699.

[15]Wu, J. C., Sankar, L. N., and Hsu, T. M., "Unsteady Aerodynamics of an Airfoil Encountering a Passing Vortex," AIAA Paper 85-0203, Jan. 1985.

[16]Hardin, J. C., and Lamkin, S. L., "Aeroacoustic Interaction of a Distributed Vortex with a Lifting Joukowsky Airfoil," AIAA Paper 84-2287, Oct. 1985.

[17]Wu, J. C., Hsu, T. M., Tang, W., and Sankar, L. N., "Viscous Flow Results for the Vortex-Airfoil Interaction Problem," AIAA

Paper 85-4053, Oct. 1985.
[18]Caradonna, F. X., Desopper, A., and Tung, C., "Finite-Difference Modeling of Rotor Flows Including Wake Effects," NASA TM-84280, 1982.
[19]McCroskey, W. J., and Goorjian, P. M., "Interactions of Airfoils with Gusts and Concentrated Vortices in Unsteady Transonic Flow," AIAA Paper 83-1691, July 1983.
[20]Jones, H. E., "The Aerodynamic Interaction Between an Airfoil and a Vortex in Transonic Flow," Workshop on Blade-Vortex Interactions, NASA Ames Research Center, Oct. 1984.
[21]Sankar, L. N. and Malone, J. B., "Unsteady Transonic Full Potential Solutions for Airfoils Encountering Vortices and Gusts," AIAA Paper 85-1710, July 1985.
[22]Srinivasan, G. R., McCroskey, W. J., and Kutler, P., "Numerical Simulation of the Interaction of a Vortex with a Stationary Airfoil in Transonic Flow," AIAA Paper 84-0254, Jan. 1984.
[23]Srinivasan, G. R., "Computations of Two-Dimensional Airfoil-Vortex Interactions," NASA CR-3885, 1985.
[24]Srinivasan, G. R., and McCroskey, W. J., "Numerical Simulations of Unsteady Airfoil-Vortex Interactions," *Vertica*, Vol. 11, No. 1/2, 1987, pp. 3–28.
[25]Milne-Thomson, L. M., *Theoretical Hydrodynamics*, 5th ed., Macmillan Press, New York, 1968.
[26]Wagner, H., "Uber die Entstehung des dynamischen Auftriebes von Tragflueln," *Zeitschrift für Angewadte Mathematik und Mechanik*, Vol. 5, No. 1, 1925, pp. 17–35.
[27]Theodorsen, T., "General Theory of Aerodynamic Instability and the Mechanism of Flutter," NACA TR 496, 1935.
[28]Straus, J., Renzoni, P., and Mayle, R. E., "Airfoil Pressure Measurements During a Blade-Vortex Interaction and a Comparison with Theory," AIAA Paper 88-0669, Jan. 1988.
[29]Renzoni, P., "Discrete Vortex Modeling of a Blade-Vortex Interaction," Ph.D. Thesis, Rensselaer Polytechnic Inst., Troy, NY, 1987.